Semicond. Sci. Technol. **23** (2008) 085004 (3pp) doi:10.1088/0268-1242/23/8/085004

Bandgap dependence of current crowding effect in 3–5 μm InAsSb/InAs planar light emitting devices

V K Malyutenko, A V Zinovchuk and O Yu Malyutenko

Lashkaryov Institute of Semiconductor Physics, 03028 Kiev, Ukraine

E-mail: malyut@isp.kiev.ua

Received 4 April 2008, in final form 16 May 2008
Published 13 June 2008
Online at stacks.iop.org/SST/23/085004

Abstract

Electroluminescence power profiles and 2D micropatterns have been obtained from InAsSb/InAs planar LEDs tuned at several wavelengths within the 3–5 μm band. Light confined to a small region around the top opaque contact was observed (cw mode, $I > 10$ mA, $T = 300$ K). A computer simulation showed that the reason behind the decrease of the emitting area is the current crowding that ensures non-uniform injection into the active region. The effect becomes more apparent in longer wavelength devices (emitting areas of 3.4 and 4.2 μm emitting devices are related as $>10:1$), providing direct evidence that the current crowding is affected by the bandgap energy of an active layer.

1. Introduction

A key challenge for infrared (IR) light emitting diode (LED) development is in accessing power output >10 mW in the 3–5 μm band, where a potential exists for applications in dynamic IR scene projection technology [1, 2]. To this end, IR LEDs have attracted a lot of attention due to a very short time constant, the ability to simulate cold [3, 4] and hot scenes and easy fabrication. These devices form a platform for photonic 'synthetic' scene projectors that are capable of competing with advanced thermal microemitter technology [5] in testing IR sensors, including forward-looking missile warning systems, search-and-track devices and missile seekers. However, the current generation of IR LEDs enables power outputs of about 1 mW at room temperature [6], and, therefore, these devices cannot simulate targets with hot engine exhausts or rocket plumes. One reason that limits the output power of IR LEDs is the non-radiative Auger recombination of carriers. This process ensures the internal quantum efficiency of uncooled devices to be as low as 20% (<0.03% the external efficiency due to refractive losses at a flat LED surface [7]), causes sub linear light-current dependences [2], and makes LEDs operate at high current density only in a pulsed mode. The attempts to increase the power emitted by scaling up dimensions of the junction area do not boost the output significantly because of a problem posed by 'current crowding' (CC). In planar structures, the CC manifests itself by forming a region of high current density in the vicinity of the top contact [8–10], resulting in a reduction of the effective emitting area [2, 10] and the local overheating of a structure [2, 10, 11]. As a result, this phenomenon causes the internal quantum efficiency to decrease [12, 13] as well as a catastrophic degradation of the device [14]. Since the reason behind the CC lies in the interaction of the lateral current component with the sheet resistances of a many-layer diode structure, numerous efforts in minimizing CC are focused on the resistance and thickness of the substrate, cladding or spreading layer, as well as contact geometry. Contrary to this tendency, in what follows, the CC is analyzed in terms of the bandgap energy E_g of the active layer in LEDs that are tuned at several wavelengths within the 3–5 μm band. We show both theoretically and experimentally that the CC is most pronounced in the longer-wavelength emitting devices, making the conventional planar LED design inefficient for application to fields that require intense IR light.

2. Experiment

The LEDs obtained from an industrial manufacturer were InAsSbP/InAsSb double heterostructures grown on 200 μm thick p-InAs substrates ($p_s \sim 10^{18}$ cm^{-3}) by liquid phase epitaxy. The structures consisted of a 0.5 μm thick p-InAsSbP confining ($p_c \sim 10^{17}$ cm^{-3}) layer, a 2 μm thick n-InAsSb active ($n_a \sim 2 \times 10^{16}$ cm^{-3}) layer and a 5 μm

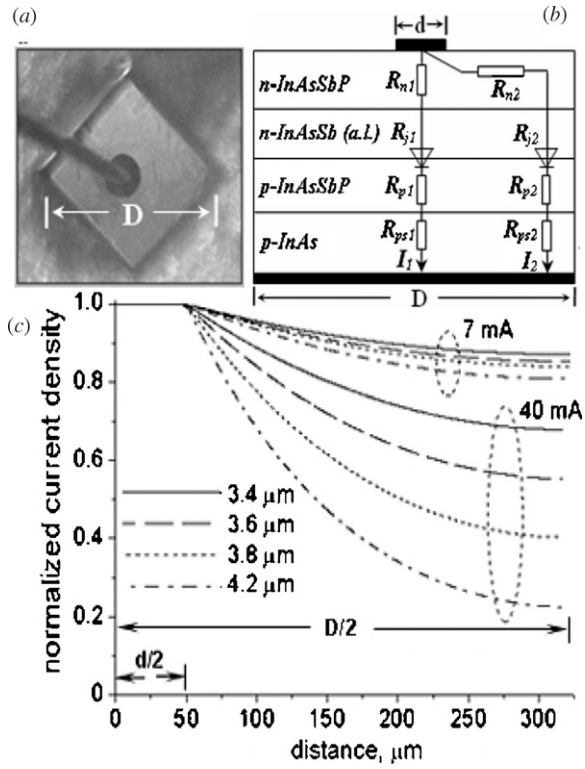

Figure 1. (*a*) Micrograph of an LED with the top point p-contact, (*b*) equivalent circuit model, real layer thicknesses are shown in the text and (*c*) current density profiles in devices tuned at different λ_p (along the diagonal crossing, theory).

thick n-InAsSbP confining ($n_c \sim 2 \times 10^{17}$ cm^{-3}) transparent layer. Their advantage consisted of the fact that the peak-emitting wavelength (λ_p) could be tailored over a 3–5 μm band only by changing the Sb content (which determines the bandgap value) in the active layer. The emitting chip (figure 1(*a*)) was packaged into the TO-39 case as a substrate-down planar 450 μm square structure with a top centrally-located metal contact (d = 100–150 μm). The point of interest lies in the lateral distribution of current in the active layer (computer simulation) and spatial non-uniformity of light (experimental micro mapping) in the devices tuned at different λ_p and operating in the pulsed mode (160 ms pulse duration) at $T \sim 300$ K. The light pattern in four LEDs (λ_p = 3.4, 3.6, 3.8, 4.2 μm) was mapped by a test system based on an IR camera operating in a 3–5 μm band while Joule heating was monitored by an 8–12 μm camera. Used in conjunction with an IR microscope, this two-band set-up has been routinely achieving the 10 μm lateral scanning step [2, 8]. To minimize the LEDs overheating caused by the CC and non-radiative recombination (<0.1 °C), the study was limited by the 40 mA bias current which is a recommended value for the cw mode.

3. Model

The lateral distribution of current density in the active layer of a device was simulated using the finite-element approach. It was assumed that the electric charges are localized in the space-charge region of the junction, that the other regions of a structure are neutral, and that the diffusion component of the current may be neglected. Therefore, the potential distribution follows from the Laplace equation, while the local current density is connected to the potential gradient via the Ohm law. The p–n junction was represented as a laterally distributed nonlinear resistor (R_j) with a diode-like current–voltage (I–V) dependence $I = I_0[\exp(V_j/mV_T) - 1]$, where I_0 is the saturation current, V_j the voltage drop across the junction, m the ideality factor and V_T the thermal voltage. The contact resistance was ignored and the condition $m = 1$ was supposed to be valid. In such approximations, the only difference between the structures tuned at different λ_p was the I_0 value that is connected to the square of intrinsic carrier concentration n_i with the concentration being dependent on a material bandgap energy $\left(I_0 \sim n_i^2 \sim \exp(-E_g)\right)$.

Figure 1(*b*) shows the cross-section of an LED structure and two possible current paths from the n to p contact. As $R_{n1} < R_{n2}$, $R_{p1} + R_{ps1} = R_{p2} + R_{ps2}$, then the voltage drop across the junction 1 is higher than that of the junction 2. Due to the nonlinear nature of the junction resistance, the inequality $R_{j1} < R_{j2}$ becomes valid at $V_{j1} > mV_T$. Moreover, the higher the forward-biased voltage, the more preferable is the vertical current path ($I_1 > I_2$) and the current crowds more effectively under the top contact.

4. Results and discussion

The lateral distribution of the current density in the active region of LEDs tuned at different λ_p is shown in figure 1(*c*). There are two specific features in this figure. At a low forward bias ($I < 10$ mA), the CC effect is negligible in all LEDs and the current spreads practically over the whole emitting region; the current density at the perimeter is only 7–12% less (depending on the E_g) than that in the center. This is due to the fact that at a low voltage the relation $R_{j1} \cong R_{j2}$ remains valid (there is no junction barrier and depletion length modulation) and of the two current routes the central one is only slightly preferable since $R_{n1} \leqslant R_{n2}$. At a higher bias, a stronger dependence of the CC on the injection current comes from the nonlinear resistance of a junction that exponentially decreases when the voltage increases. As $V_{j1} > V_{j2}$, it is apparent that the higher the applied voltage, the stronger is the inequality $R_{j1} < R_{j2}$, and the central current route through the junction 1 becomes more preferable; at $I = 40$ mA, the current density at the perimeter of the emitting area decreases by 1.5–4.5 times. Most important is that at the longer wavelength emitting devices, the CC effect is stronger and the magnitude of the injection current at the perimeter of a device is much lower. This trend is the direct effect of the dependence of the junction resistance on a material bandgap: at a longer wavelength emitting LED with a lower junction resistance, the n-confining layer cannot serve simultaneously as a spreading layer.

Figure 2 illustrates how the CC modifies the light pattern and prevents IR LEDs from having a large emitting area. Shown in figure 2(*a*) is the diagonal crossing of light emitted by several devices at $I = 40$ mA. The central dip at the curves and maps is due to the top contact that prevents some of the light from passing through the contact area while the non-zero

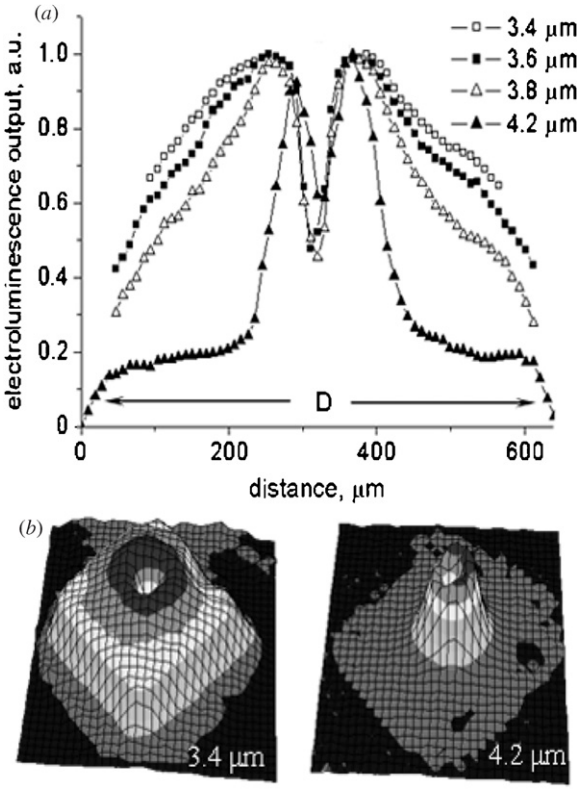

Figure 2. (*a*) Experimental electroluminescence power profiles in LEDs with different λ_p (note, the diameters of top contacts are slightly different) and (*b*) spatial view of the power emitted. All the tests are taken at $I = 40$ mA.

signal in the dip is due to reflection of a Lambertian light pattern by the contact. When conditionally determined as the distance from the center of the top contact to the position of half maximum of power emitted, the CC lengths were >300, 300, 220, and only 100 μm for the devices emitting at 3.4, 3.6, 3.8 and 4.2 μm, respectively. Such light that is confined to a small region around the top non-transparent contact causes the emitting area to catastrophically decrease in longer wavelength devices (figure 2(*b*)). When subtracting the size of the top contact platform, the effective emitting area is compared with a LED surface in both of the shorter wavelength emitting devices, but it decreases by half (48%) in 3.8 μm LEDs and finally reduces to 7% in 4.2 μm LEDs.

Of two ways toward increasing the emitting area in longer wavelength LEDs (increasing the doping density or the thickness of the n-type confining layer), layer thickness control appears to be preferable.

5. Conclusions

This study has provided direct evidence of the material bandgap effect on the CC in 3–5 μm InAsSb/InAs planar LEDs through the observation of spatial non-uniformity of light in the micro scale. It has been experimentally demonstrated that in structures with a centrally located top contact, the modification of the light pattern by the CC cannot be neglected even at current as low as 40 mA which is a recommended value for cw operation. This pure electronic effect that is connected to the nonlinear resistance of p–n junction drastically affects the performance of red-shifted LEDs. Our calculations and tests have shown that devices made of a narrower bandgap material ($\lambda_p = 4.2$ μm) have much less uniform injected current density, compared to those with a wider bandgap value ($\lambda_p = 3.4$ μm). Therefore, this leads to a catastrophic decrease in the effectively emitting area (emitting areas of 3.4 and 4.2 μm emitting devices are related as >10:1) as well as a higher local heating in red-shifted devices. Finally, the lateral thermal gradient may cause thermal lensing and uncontrollable deformation of the light pattern. Such observations can lead to an improved device design with a larger emitting area, more uniform current density in the confining layers, a lesser thermal gradient in the active region and, lastly, a higher efficiency at an extreme operation mode. In our opinion, the room for improvement is limited due to the trade-off between CC impact and optical transparency of the top confining layer. The calculation shows that for 4.2 μm LEDs the five-fold increase in doping level or thickness of the layer causes only slightly uniform current spreading ($I_d/I_D = 2.25$ compared to $I_d/I_D = 5$ in the LED under test). However, it results in the five-fold increase of absorption coefficient due to activation of the free carrier absorption.

Acknowledgment

The authors gratefully acknowledge financial support by the Ministry of Education and Science within the Ukrainian–Russian Nanotechnology Project (contract M/190-2007).

References

[1] Das N C, Olver K, Towner F, Simonis G and Shen H 2005 *Appl. Phys. Lett.* **87** 041105
[2] Malyutenko V K, Malyutenko O Yu and Zinovchuk A V 2006 *Appl. Phys. Lett.* **89** 201114
[3] Malyutenko V 2004 *Physica* E **20** 553
[4] Lindle J R, Bewley W W, Vurgaftman I, Meyer J R, Thomas M L, Piquette E C, Edwall D D and Tennant W E 2007 *Appl. Phys. Lett.* **90** 241119
[5] Robinson R, Oleson J, Rubin L and McHugh S 2000 *Proc. SPIE* **4027** 387
[6] Sherstnev V V, Monakhov A M, Krier A and Hill G 2000 *Appl. Phys. Lett* **77** 3908
[7] Kane M J, Braithwaite G, Emeny M T, Lee D, Martin T and Wright D R 2000 *Appl. Phys. Lett.* **76** 943
[8] Matveev B A, A'daraliev M, Zotova N V, Karandashev S A, Remenniy M A, Stus' N M, Talalakin G N, Malyutenko V K and Malyutenko O Yu 2001 *Proc. SPIE* **4285** 109
[9] Malyutenko V K, Malyutenko O Yu, Podoltsel A D, Kucheryavaya I N, Matveev B A, Remennyi M A and Stus' N M 2001 *Appl. Phys. Lett.* **79** 4228
[10] Malyutenko V K, Malyutenko O Yu, Dazzi A, Gross N and Ortega J M 2003 *J. Appl. Phys.* **93** 9398
[11] Monakhov A, Krier A and Sherstnev V V 2004 *Semicond. Sci. Technol.* **19** 480
[12] Kettle J, Perks R M and Dunstan P 2006 *Electron. Lett.* **42** 1122
[13] Guo X and Schubert E F 2001 *Appl. Phys. Lett.* **78** 3337
[14] Malyutenko V K, Malyutenko O Yu, Zinovchuk A V, Zakheim A L, Zakheim D A, Smirnova I P and Gurevich S A 2005 *Proc. SPIE* **5941** 59411K